Optical characterization of polychromatic organic light emitting diodes

David Troadec, André Moliton, Bernard Ratier, Rémi Antony, Roger C. Hiorns

Optical characterization of polychromatic organic light emitting diodes

David Troadec, André Moliton, Bernard Ratier, et al.

View Online

Export Citation

Optical characterization of polychromatic organic light emitting diodes

David Troadec, André Moliton,[a] Bernard Ratier, and Rémy Antony
Unite de Microelectronique Optoelectronique et Polymeres CNRS—FRE 2701, Faculté des Sciences et Techniques, 123 Av. Albert Thomas, 87060 Limoges, France

Roger C. Hiorns
LPCP, CNRS UMR-5067, 2 Avenue du Président Angot, 64053 Pau, France

Luminance and quantum yields of organic light emitting diodes (OLEDs) are generally calculated by using a hypothetic monochromatic emission even though the actual external emission is lower than the internal emission because of internal reflection, and is polychromatic. For organic materials, we present the effects of the total internal reflection on quantum yields. Calculations for the luminance and the efficiency of an ideal pseudomonochromatic source are compared with those for a real polychromatic source. While we demonstrate that the calculation of the yield is practically unchanged whatever hypothesis is used, we do show, however, that by assuming that the source is pseudomonochromatic, the luminances of green and blue OLEDs are overvalued or undervalued by a factor of 4, respectively. © *2005 American Institute of Physics*. [DOI: 10.1063/1.1835538]

I. INTRODUCTION

The ability of molecular and macromolecular organic materials to be deposited on virtually any substrate, including those which are flexible, has solicited considerable research into their use as replacements for inorganic semiconductors in a wide range of applications. However, for a considerable period of time, the minimum tension (the work voltage) required to produce electroluminescence of these organic materials was found to be too high for their general use. A good example is that of anthracene which demanded the application of around 100 V to operate[1,2] due to the thickness of the available crystals. Nevertheless, over the last 15 years, the emergence of materials based on molecules such as 8-tris-hydroxyquinoline aluminium (Alq_3) (Ref. 3) or on π-conjugated polymers such as poly(*para*-phenylene vinylene) (PPV) (Ref. 4) has resolved this problem by permitting the preparation of thin films, respectively, *via* evaporation and spin-coating techniques. More recently there has been a tremendous growth in the use of organic light emitting diodes (OLEDs) for pixel technology, stimulated by the economic gains available to display manufacturers.

In this article, we focus our interest on the photometric characterization of these OLEDs by comparing the luminance and yields of OLEDs emitting either green or blue light. We aim to clarify how the determination of luminance using a polychromatic "configuration" in place of the more classically used monochromatic system permits a more complete characterization of blue OLEDs which in principle tend to exhibit lower luminances than their green counterparts.

For the green OLEDs we used as the emitter the molecule Alq3 which has its structure shown in Fig. 1(a). In place of the more commonly used structure based on a single active layer sandwiched between a transparent indium tin oxide anode on glass and a calcium/aluminium alloy cathode, i.e., indrum tin oxide (ITO)/Alq3/Ca+Al, we used heterostructure OLEDs which resulted in improved characteristics. For the most part, they were layered in the order ITO/poly(3,4-oxyethyleneoxythiophene) blended with poly(styrene sulfonate) (PEDOT-PSS)/N,N'-bis(3-methylphenyl)-N,N'-diphenyl benzidine (TPD)/Alq3/Ca+Al. The PEDOT-PSS, detailed in Fig. 1(b), and the TPD, detailed in Fig. 1(c), were used as hole injection (HIL) and hole transport layers (HTL), respectively. For blue OLEDs, we used the metal chelate Zn(bis-salen-4)$_2$ detailed in Fig. 1(d) for the active layer along with TPD or polyvinylcarbazole (PVK) or copper phthalocyanine (CuPc) as HTLs. These materials were used in improved albeit more complex structures, e.g., ITO/TPD/Zn(bis-salen-4)$_2$/Ca+Al, or ITO/PVK/Zn(bis-salen-4)$_2$/Ca+Al). It should be noted that
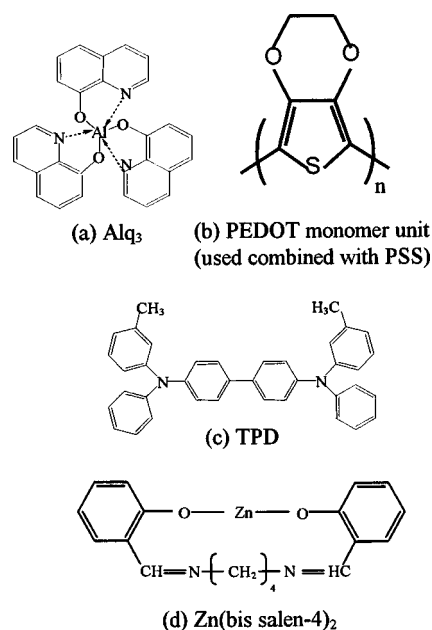

FIG. 1. Chemical structures of molecules used in OLEDs.

[a] Author to whom correspondence should be addressed; electronic address: amoliton@unilim.fr

the monolayer structure ITO/Zn(bis-salen-4)$_2$/Ca+Al remains quite common.[5] While more complicated structures have been investigated,[6–10] the aim of this article is to present a general optical characterization of OLEDs which can be applied whatever the physical or chemical structure of the device. It is for this reason that we have characterized the optoelectronic properties of different structures based on either ITO/HTL/Alq3 or Zn(bis-salen-4)$_2$/Ca+Al or ITO/HTL/HIL/Alq3 or Zn(bis-salen-4)$_2$/Ca+Al layers with widely available photodiodes and standard laboratory apparatus.

II. PHOTOMETRIC CHARACTERIZATION OF OLEDS

In general, luminance calculations are performed taking into account a characterizations of the device at its maximum emission wavelength (λ_{max}) only. The emitted spectrum is thus assumed to be monochromatic. However, the majority of OLEDs exhibit wide emission spectra, a specific characteristic of OLEDs.[2]

The spectral distribution of the energetic flux $[\Phi'_e(\lambda)]$ is defined by $\Phi'_e(\lambda) = \lim_{\delta\lambda \to 0}(\delta\Phi_e/\delta\lambda)$, in which a fraction of the energetic flux ($\delta\Phi_e$) is found within a spectral bandwidth ($\delta\lambda$) around a certain wavelength (λ).[11,12] In practice, to calculate $\Phi'_e(\lambda)$ from the total flux Φ_e, we have to measure the normalized electroluminescent spectrum $[S(\lambda)]$, as in

$$\Phi'_e(\lambda) = \frac{\Phi_e S(\lambda)}{\int_0^\infty S(\lambda)d\lambda}. \tag{1}$$

For a monochromatic source (emission at λ_d), the relation between energetic and luminous values of the flux (Φ_e and Φ_v, respectively) is classically written

$$\Phi_v(\lambda_d) = K_m V(\lambda_d)\Phi_e(\lambda_d), \tag{2}$$

in which $K_m = 683$ lm W^{-1}. It should be noted that $V(\lambda)$ is a normalization with respect to the difference between the actual luminance and that observed by the eye at different wavelengths.

For a polychromatic source, the spectral value $[\Phi'_v(\lambda)]$ can be defined using the total flux included within the spectral band under consideration (λ_a, λ_b), so that $\Phi_v \overset{\text{def}}{\equiv} \Phi_v(\lambda_a, \lambda_b) = \int_{\lambda_a}^{\lambda_b}\Phi'_v(\lambda)d\lambda$. As $\Phi'_v(\lambda)$ can be expressed using the general exchange between luminous and energetic values, the luminous flux is given by

$$\Phi_v = \int \Phi'_v(\lambda)d\lambda = K_m \int V(\lambda)\Phi'_e(\lambda)d\lambda. \tag{3}$$

Other photometric values, such as energetic luminance (L_e) and luminous luminance (L_v), or the energetic intensity (I_e), and luminous intensity (I_v), are defined similarly from the energetic (Φ_e) and luminous (Φ_v) fluxes

$$L_e = \frac{\Phi_e}{\Omega S_a} \tag{4a}$$

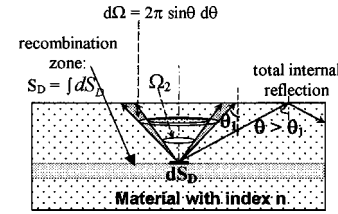$$\text{and } L_v = \frac{\Phi_v}{\Omega S_a}, \tag{4b}$$

FIG. 2. Schematization showing how only certain emitted rays are allowed to escape to the exterior due to the critical solid angle $\Omega_2 = 2\pi[1 - \cos\theta_1]$.

$$I_e = \frac{\Phi_e}{\Omega} \tag{5a}$$

$$\text{and } I_v = \frac{\Phi_v}{\Omega}, \tag{5b}$$

in which Ω is the solid angle of the emission shown in Fig. 2 and S_a the projected area of the source. The flux is assumed constant in these definitions. In addition, for each L_e, L_v, I_e, and I_v, analogous relations to Eqs. (1)–(3) exist.

III. INTERNAL AND EXTERNAL FLUXES, QUANTUM YIELDS, AND THE CORRESPONDING OLEDS EMISSIONS

A. Restrictions limiting the passage of an internal ray to the exterior of an OLED

Figure 2 schematizes the emission from an OLED toward the exterior. The ray emitted by the emitting layer reaches the organic phase and air interface at an angle of incidence (θ) which can be greater or less than the critical angle (θ_1) which is defined by the relationship $n\sin\theta_1 = n_{air} = 1$, where n is the refractive index of the organic material. When $\theta < \theta_1$, the flux is transmitted to the exterior, however, when $\theta > \theta_1$, the flux undergoes a total internal reflection and is, *a priori*, returned back into the OLED structure without reaching the exterior.

1. Neglected effects

When $n=2$, we have $\theta_1 \approx 30°$. This being a relatively small incident angle, not far from the normal incidence, means that we can use the reflection coefficient (R) in the form $R \approx (n-1/n+1)^2$, which yields a transmission coefficient of $T = 1 - R \approx 75\%$. However, if $n=1.5$, then $T \approx 96\%$, and $\theta_1 \approx 40°$, which in turn renders the use of the equation $R \approx (n-1/n+1)^2$ debatable. Given the relatively low indexes that organic materials exhibit, T is generally accepted without correction and is approximated to $T \approx 100\% = 1$ when $\theta < \theta_1$. Furthermore, given that variations in the index with wavelength are small within the limited range of optical wavelengths under study, and little dispersion occurs along with a weak absorption, we can assume that the index is a constant.

2. Effects due to the critical angle

As shown in Fig. 2, the critical angle imposes a restriction on the emitted rays so that only those at an angle $\theta < \theta_1$ reach the exterior of the structure. So
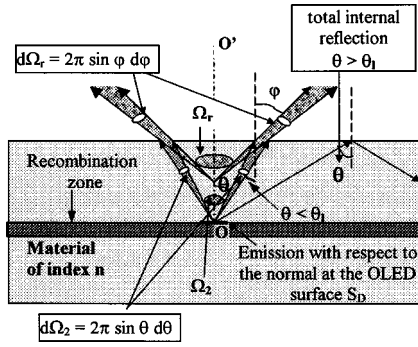
FIG. 3. Internal and external emissions of an OLED.

- At the OLED interior, in the recombination zone, emissions going toward the frontal surface occur in a half space, that is $\Omega_1 = 2\pi$, and
- The portion of flux which can leave the OLED is emitted from the emission zone within a solid angle limited to $\Omega_2 = 2\pi \int_{\theta=0}^{\theta=\theta_1} \sin\theta \, d\theta = 2\pi(1 - \cos\theta_1)$.

Given that $\sin\theta_1 = 1/n$, the term $C = [1 - \cos\theta_1]$ can be approximated as follows:

$$C = [1 - (1 - \sin^2\theta_1)^{1/2}]$$
$$= \left[1 - \left(1 - \frac{1}{n^2}\right)^{1/2}\right]$$
$$\approx \left[1 - \left(1 - \frac{1}{2n^2}\right)\right]$$
$$= \frac{1}{2n^2}. \tag{6a}$$

We finally obtain $\Omega_2 = \pi/n^2$, from which we can deduce

$$\Omega_2 = \frac{\Omega_1}{2n^2}. \tag{6b}$$

From Eq. (6a) and (6b), we can see that the solid angle at the exterior (Ω_2) is only a fraction of the total emission angle (Ω_1) and that external yields are considerably affected. In effect, the external flux is only a fraction of that emitted by the active layer, and is wavelength independent if we assume—as previously mentioned in Sec. III A 1—that the index is also wavelength independent.

B. Isotropic internal and external emissions according to Lambert's law

This section is limited to considering a ray incident to the material/air interface with $\theta < \theta_1$. Refraction laws modify the geometry of the solid angle cones of the emission, as schematized in Fig. 3. Now, $n \sin\theta = \sin\varphi$, and differentiation yields $d\theta/d\varphi = \cos\varphi/n\cos\theta$. As $n\cos\theta = \sqrt{n^2(1 - \sin^2\theta)}$, or from the Snell–Descarte law, $n\cos\theta = \sqrt{(n^2 - \sin^2\varphi)}$, we obtain $d\theta/d\varphi = \cos\varphi/\sqrt{(n^2 - \sin^2\varphi)}$. The elementary solid angles $d\Omega_2$ and $d\Omega_r$, defined in Fig. 3, are such that $d\Omega_2/d\Omega_r = \sin\theta/\sin\varphi \, d\theta/d\varphi = 1/n \cos\varphi\sqrt{(n^2 - \sin^2\varphi)}$.

For organic materials, $n \approx 2$ and $\sin^2\varphi$ is well below 1. Therefore, $\sin^2\varphi \ll n^2$ and we have

$$\frac{d\Omega_2}{d\Omega_r} \approx \frac{\cos\varphi}{n^2}. \tag{7}$$

Equation (7) indicates that a ray emitted directly toward the exterior, at a solid angle Ω_2, is in approximate accord with Lambert's law.[13]

C. Determination of internal and external emitted fluxes

It should be noted that the calculations here concern only fluxes emitted toward the front of the device.

1. Total internal flux emitted inside the structure

Assuming the material to be homogeneous and having no interface, the internal emission from the recombination zone is isotropic and the total emitted flux inside the forward half space can be written in the following form:

$$\Phi_{T\,int} = \int_{1/2\mathrm{space}} I_{0\,int} d\Omega = 2\pi \, I_{0\,int}, \tag{8}$$

in which as $I_{0\,int}$ represents the luminous intensity directly emitted by the source.

2. Fraction of total internal flux emitted towards the exterior

Again, the luminous intensity $I_{0\,int}$ is isotropic in nature. However, the emission angle is limited to θ_l, as explicitly detailed in Sec. III A. By denoting Φ_{ie} as the flux from the interior toward the exterior, we have

$$\Phi_{ie} = 2\pi \, I_{0\,int} \int_0^{\theta_l} \sin\theta \, d\theta = 2\pi \, I_{0\,in}(1 - \cos\theta_l)$$

$$\overset{(6')}{=} 2\pi \, I_{0\,in} \frac{1}{2n^2} = \pi \, I_{0\,in} \frac{1}{n^2} \overset{(8)}{=} \Phi_{T\,int} \frac{1}{2n^2}. \tag{9}$$

3. Emitted exterior flux

As we have already seen, the emission follows Lambert's law, so that $I_{ext} = I_{0\,ext} \cos\varphi$, where $I_{0\,ext}$ is the luminous intensity emitted with respect to the normal of the surface of the OLED. The total external flux (Φ_{ext}) emitted over the forward half space is thus in the following form:

$$\Phi_{ext} = \int_{1/2\mathrm{space}} I_{0\,ext} \cos\varphi \, d\Omega$$

$$= 2\pi \, I_{0\,ext} \int_0^{\pi/2} \cos\varphi \sin\varphi \, d\varphi$$

$$= 2\pi \, I_{0\,ext} \int_0^1 \sin\varphi \, d(\sin\varphi) = \pi \, I_{0\,ext}. \tag{10}$$

4. Relationships between fluxes

Given that the emitted external flux is a fraction of the total internal emitted flux, conserving the overall beam power, we have $\Phi_{ie} = \Phi_{ext}$. This gives $I_{0\,in} = n^2 I_{0\,ext}$, and also
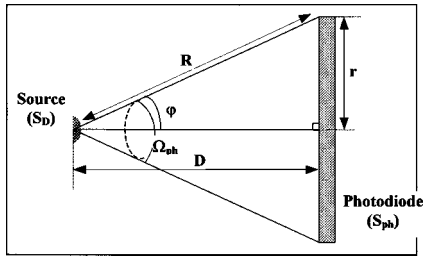
FIG. 4. Simplified schematization of diode/photodiode.

$$\Phi_{\text{ext}} = \frac{1}{2n^2} \Phi_{T\,\text{int}}.\tag{11}$$

The factor $1/2n^2$ represents the actual or "optical" yield of rays emitted from the OLED; as n is small in organic materials (typically $n \leqslant 2$), $1/2n^2$ is high along with the optical yield, especially when compared to inorganic devices.

5. External and internal quantum yields

The external quantum yield (η_{ext}) is defined as the ratio of the number (N_{ext}) of photons emitted by a diode into the external half space over a time t divided by the number of electrons flowing in the external circuit (N_{el}) during the same period of time.

η_{ext} can be expressed therefore by the relationship

$$\eta_{\text{ext}} = \frac{N_{\text{ext}}}{N_{\text{el}}}.\tag{12}$$

If I_c represents the current injected into an electroluminescent structure, then $I_c = N_{\text{el}}q/t$, where q is the value of the elementary charge ($q = 1.6 \times 10^{-19}$ C). However, for a given wavelength (λ_d), the energy of the photons is determined by $E_{\text{ph}} = hc/\lambda_d$, and thus $N_{\text{ext}}/t = \lambda_d/hc\Phi_{\text{ext}}$. So, for a pseudomonochromatic ray, Eq. (12) gives

$$\eta_{\text{ext}} = \frac{q\lambda_d}{hc} \frac{\Phi_{\text{ext}}}{I_c}.\tag{13}$$

By analogy, we find for the internal quantum yield that $\eta_{\text{int}} = q\lambda_d/hc\Phi_{\text{int}}/I_c$, and with Eq. (11)

$$\eta_{\text{ext}} = \frac{1}{2n^2} \eta_{\text{int}}.$$

IV. MEASURING MONOCHROMATIC AND POLYCHROMATIC LUMINANCE AND YIELDS WITH A PHOTODIODE

A. Sensitivity and spectral sensitivity of a photodiode

1. Basic formula

If I_{ph} is the current intensity through the photodiode, which acts as photon detector for the organic diodes which do not necessarily emit only monochromatic light, we have

$$I_{\text{ph}} = I_0 + I_p,\tag{14}$$

in which I_0 is the dark current and I_p the photoelectric current. Normally, if conditions remain unchanged during characterization, I_0 remains constant and I_p changes with the re-
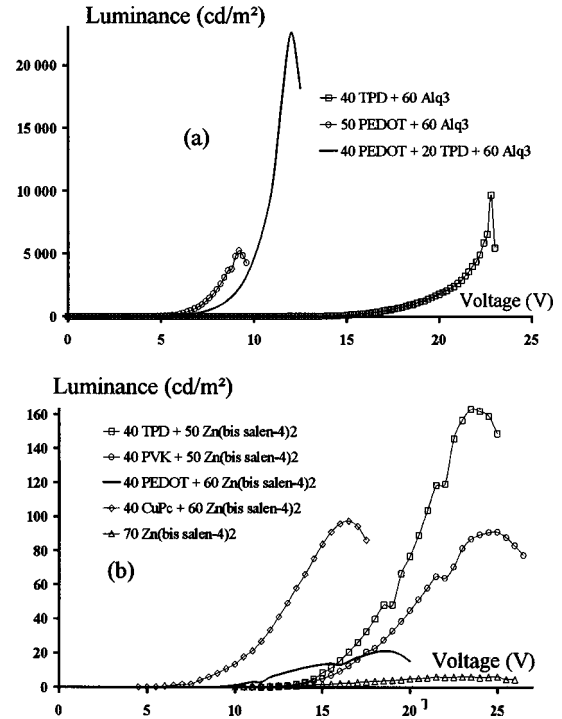
FIG. 5. $L(V)$ characteristics of (a) green; and (b) blue OLEDs.

ceived flux Φ_e. Whatever the photodetector, its sensitivity σ is defined by its characteristic slope, i.e.,

$$\sigma = \frac{dI_{\text{ph}}}{d\Phi_e}.\tag{15a}$$

For a linear photodetector, where I_p changes proportionally with Φ_e, then

$$\sigma = \frac{I_p}{\Phi_e}.\tag{15b}$$

The spectral sensitivity, to a monochromatic ray of light with wavelength λ, is defined by the relationship

$$\sigma(\lambda) = \frac{dI_p(\lambda)}{d\Phi_e(\lambda)} = \frac{I_p'(\lambda)}{\Phi_e'(\lambda)}.\tag{16}$$

If the light is polychromatic, the current I_p is therefore such that

$$I_p = \int dI_p \overset{(16)}{=} \int \sigma(\lambda)d\Phi_e(\lambda) = \int \sigma(\lambda)\Phi_e'(\lambda)d\lambda$$

$$= \int I_p'(\lambda)d\lambda.\tag{17}$$

We thus have:

$$\frac{I_p}{\Phi_e} = \frac{\int \sigma(\lambda)\Phi_e'(\lambda)d\lambda}{\Phi_e} \overset{(1)}{=} \frac{\int \sigma(\lambda)S(\lambda)d\lambda}{\int S(\lambda)d\lambda} = \sigma_{\text{av}};\tag{18}$$

and the value σ_{av} then obtained for the ratio I_p/Φ_e appears as an effective or average sensitivity defined by Eq. (18). Fur-

TABLE I. Optoelectronic performances of various structures with Alq3 as emitter.

Structures	$V_{Threshold}$ (V)	η_{ext} (%)	L_{max} (cd m^{-2})
ITO/40 nm TPD/60 nm Alq3/Ca+Al	8.6	0.68	9660
ITO/50 nm PEDOT/60 nm Alq3/Ca+Al	11.0	0.64	4385
ITO/40 nm PEDOT/20 nm TPD/60 nm Alq3/Ca+Al	3.5	0.85	22 500

thermore, Eq. (18) also gives: $\Phi_e = I_p[\int S(\lambda)d\lambda / \int \sigma(\lambda)S(\lambda)d\lambda]$; with Eq. (1) we finally have:

$$\Phi'_e(\lambda) = I_p \frac{S(\lambda)}{\int \sigma(\lambda)S(\lambda)d\lambda}. \tag{19}$$

2. Example photodiode set-up

Photometric measurements are typically performed using a photodiode with as large a surface area as possible, for example, of the order of 100 mm^2.

The classic set-up for measuring luminance with a photodiode. In general terms, the measurement of a beam emitted by an OLED is effected by placing a photodiode at the window of the measuring cell, as shown in Fig. 4. The surface of the photodiode is perpendicular to the beam direction, so if the surface of the OLED is denoted by S_D, the apparent surface (S_a) is such that $S_a = S_D$. While the surface of the photodiode (S_{ph}) can be around 1 cm^2, the surface of the OLED is closer to several mm^2. We can therefore reasonably assume that the source is a point with respect to the receptor.

The half angle at the apex (φ) is such that $\tan \varphi = r/D$. Given typical values, that is with $r \approx 5$ mm, $D \approx 40$ mm, and $\varphi \approx 7°$, the solid angle is therefore $\Omega = \Omega_{ph} \approx 0.05$ sr. The coefficient $1/\Omega S_a$, which appears with equal use in Eqs. (4a), (4b), (5a), and (5b) for luminance in monochromatic and polychromatic "configurations," is such that $S_a = S_D$ and $\Omega = \Omega_{ph}$.

B. Luminance

1. A monochromatic system

As detailed in Fig. 4, Ω_{ph} denotes the solid angle of the photodetector toward the organic diode, and Φ_{ph} the energetic flux received by the photodetector from the diode. In terms of monochromatic flux, from Eqs. (4) and (15b) at a given wavelength $\lambda = \lambda_d$ and $\sigma = \sigma(\lambda_d) = I_p/\Phi_{ph}$, where $\sigma(\lambda_d)$ is the spectral response of the photodiode. We can therefore state that

$$L_e = \frac{\Phi_{ph}}{\Omega_{ph}S_a} \overset{(15')}{\approx} \frac{\Phi_{ph}}{\Omega_{ph}S_D} = \frac{I_p}{\Omega_{ph}S_D\sigma(\lambda_d)}.$$

This in turn yields the luminous luminance:

$$L_v = \frac{K_m I_p}{\Omega_{ph}S_D} \frac{V(\lambda_d)}{\sigma(\lambda_d)} = \frac{K_m I_p}{\Omega_{ph}S_D}B, \quad \text{with } B = \frac{V(\lambda_d)}{\sigma(\lambda_d)}. \tag{20}$$

Equation (20) is widely used, and is even generally applied to a polychromatic source. However, when dealing with polychromatic systems, it is possible to modify the factor B to a factor which we shall denote as A. The ratio A/B gives an account of the extent of approximation required for a polychromatic source perceived as a pseudo-monochromatic source.

2. The real polychromatic case

The luminous flux L_v is given by Eq. (5) where Φ_v is expressed by Eq. (3) as a function of $\Phi'_e(\lambda)$. With Eq. (19) we thus obtain

$$L_v \overset{(5)}{=} (\Phi_v/\Omega_{ph}S_a)$$
$$\approx (\Phi_v/\Omega_{ph}S_D)$$
$$\overset{(3)}{=} (K_m/\Omega_{ph}S_a) \int V(\lambda)\Phi'_e(\lambda)d\lambda$$
$$\overset{(19)}{=} (K_m I_p/\Omega_{ph}S_D)\left[\int V(\lambda)S(\lambda)d\lambda / \int \sigma(\lambda)S(\lambda)d\lambda\right],$$

that is to say

$$L_v = \frac{K_m I_p}{\Omega_{ph}S_D}A, \quad \text{where } A = \frac{\int V(\lambda)S(\lambda)d\lambda}{\int \sigma(\lambda)S(\lambda)d\lambda} = \frac{V_{av}}{\sigma_{av}}. \tag{21}$$

[V_{av} is defined in analogy to σ_{av}, introduced in Eq. (18)].

C. Characterizing yields

The external yield is given by Eq. (13). Φ_{ext} has already been calculated using Eq. (10), and we have seen that $\Phi_{ext} = \pi I_{0 \, ext}$. With the energetic intensity given by Eq. (4b), which represents the flux within a solid angle unit, and with

TABLE II. Optoelectronic performances of various structures with Zn(bis-salen-4)$_2$ as emitter.

Structures	$V_{Threshold}$ (V)	η_{ext} (%)	L_{max} (cd m^{-2})
ITO/40 nm TPD/50 nm Zn(bis-salen-4)$_2$/Ca+Al	11.4	0.145	163
ITO/40 nm CuPc/60 nm Zn(bis-salen-4)$_2$/Ca+Al	4.7	0.095	97.5
ITO/40 nm PVK/50 nm Zn(bis-salen-4)$_2$/Ca+Al	10.5	0.24	99.8

Eq. (15b), we have for a monochromatic system: $I_{ext} = (1/\Omega_{ph})[I_p/\sigma(\lambda_d)]$. In addition, $I_{ext} = I_{0\,ext}\cos\varphi$, so with $\varphi \approx 7°$ and $\cos\varphi = 0.992 \approx 1$, $I_{ext} \approx I_{0\,ex}$ and thus $\Phi_{ext} = \pi\,I_{0\,ext} = (\pi/\Omega_{ph})[I_p/\sigma(\lambda_d)]$. Placing this into Eq. (13) we obtain

$$\eta_{ext} = \frac{q}{hc}\frac{\pi}{\Omega_{ph}}\frac{\lambda_d}{\sigma(\lambda_d)}\frac{I_p}{I_c}. \tag{22}$$

This can be also expressed in the form

$$\eta_{ext} = \frac{q}{hc}\frac{\pi}{\Omega_{ph}}\frac{I_p}{I_c}D, \quad \text{with } D = \frac{\lambda_d}{\sigma(\lambda_d)}. \tag{23}$$

By analogy, and as we verified by direct calculations, we obtain for the polychromatic system

$$\eta_{ext} = \frac{q}{hc}\frac{\pi}{\Omega_{ph}}\frac{I_p}{I_c}C, \quad \text{with } C = \frac{\displaystyle\int_0^\infty \lambda S(\lambda)\,d\lambda}{\displaystyle\int_0^\infty \sigma(\lambda)S(\lambda)\,d\lambda} = \frac{\lambda_{av}}{\sigma_{av}}. \tag{24}$$

V. A COMPARISON BETWEEN CALCULATIONS BASED ON THE MONOCHROMATIC HYPOTHESIS AND THE REAL POLYCHROMATIC SITUATION

To understand the difference between the two titled calculations, we have taken two example sets of OLEDs emitting either green or blue light.[14,15] The green OLEDs were obtained with an Alq$_3$ emissive layer, and the $L(V)$ characteristics of optimized structures (which included HILs or/and HTLs) are reported in Fig. 5(a). The optoelectronic parameters are indicated in Table I. The blue structures were based on the emitter Zn(bis-salen-4)$_2$ Figure 5(b) presents the $L(V)$ characteristics of these structures and the optoelectronic performances of the three best OLEDs are reported in Table II.

Finally, the normalized electroluminescence spectra $[S(\lambda)]$ are reported in Fig. 6(a) for the green OLEDs. In Fig. 6(b), we report the normalized electroluminescence spectrum of the typical blue structure ITO/40 nm TPD/50 nm Zn(bis-salen-4)$_2$/Ca+Al. These curves are drawn in relation to the normalized photoptical eye response $[V(\lambda)]$ and to the spectral sensitivity of the photodiode $[\sigma(\lambda_d)]$. It should be noted here that the $\sigma(\lambda_d)$ values for a standard diode range from 350 to 750 nm and were provided by Radiospares®. It is evident from these figures that $V(\lambda)$ is centered more closely to the emission of the green OLED than that of the blue OLED.

In Table III, we report the values of the A factors, calculated by numerical integration of empirical values obtained over the electroluminescent spectrum, and the B factors, which are used to yield L_v. As mentioned above, the A factor (polychromatic) takes the whole emission spectrum into account while the B factor (pseudomonochromatic) takes only
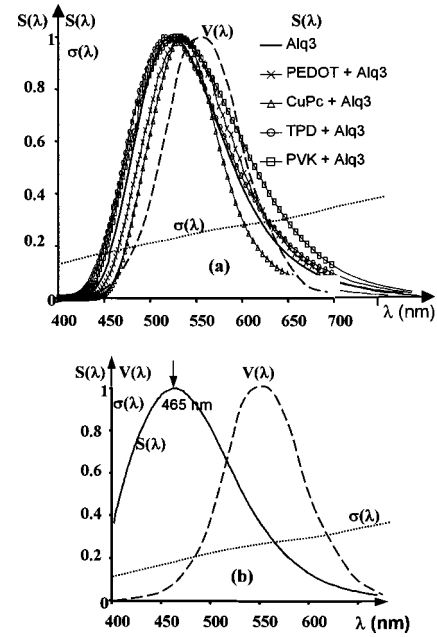

FIG. 6. (a) Normalized electroluminescence spectrum of green OLEDs drawn with respect to $V(\lambda)$ and $\sigma(\lambda)$ curves, i.e., photoptical eye response and spectral sensitivities, respectively. (b) Normalized electroluminescence spectrum of a representative blue OLED drawn with respect to $V(\lambda)$ and $\sigma(\lambda)$ curves, i.e., photoptical eye response and spectral sensitivities, respectively.

the maximum wavelength of the spectrum. In Table IV the two terms are compared for each of the OLED types:

- Green OLED (maximum emission at $\lambda_{max} = 532$ nm) with structure ITO/TPD/Alq3/Ca+Al; and
- Blue OLED ($\lambda_{max} = 465$ nm) with the structure ITO/TPD/Zn(bis salen-4)$_2$/Ca+Al.

We note that the ratio $A/B = (L_v)_{polychrom.}/(L_v)_{monochrom.}$ is not equal to 1, and is dependent on the emission color. In the case of green OLEDs, the A factor is lower than the B factor, whereas the inverse is true for the blue OLED. The classic calculation (pseudomonochromatic hypothesis) overvalues the diode luminance for the green OLEDs and undervalues the luminance of the blue OLED. Remarkably, we obtain a factor at least 4 (more precisely 4.37 according to the experimental results shown in Table III(b)) between the ratios of luminances of blue and green OLEDs calculated using both the polychromatic and the simplified monochromatic methods

$$[(L_v)_{blue}/(L_v)_{green}]_{polych} \approx 4[(L_v)_{blue}/(L_v)_{green}]_{mono}.$$

In Table III(b), and again for the two green and blue OLEDs, we report the values of the coefficients C (calculated by numerical integration) and D which are used, respectively, to obtain the η yields for polychromatic and monochromatic studies. In the two cases (green and blue OLEDs), the ratio $C/D \approx 1$ shows that the yield is—in practical terms—invariant with respect to the use of the hypothetical calculation, in opposition to the results obtained for luminance calculations.

In fact, these results should not be surprising, as the A factor [see Eq. (21)] is dependent on $V(\lambda)$ (that is, on the

TABLE III. (a) *A* (polychromatic source) and *B* (pseudomonochromatic source) factors and their ratios; and (b) *C* (polychromatic source) and *D* factors (pseudomonochromatic source) and their ratios.

Diode	(a) Luminance calculation			(b) Yield determination		
	A (lm/A)	B (lm/A)	A/B	C (nm W A^{-1})	D (nm W A^{-1})	C/D
Green	1485	2224	0.67	1963	1976	0.99
Blue	698	239	2.92	2212	2165	1.05

spectral distribution as shown in figure 6), while the *C* factor [see Eq. (24)] is independent of the diurnal photoresponse $V(\lambda)$.

VI. CONCLUSION

The photometric parameter calculations based on a pseudomonochromatic source are admittedly simpler than those required for the polychromatic configuration. However, while the calculated yield remains practically unchanged whichever hypothesis is used, the simplified pseudo-monochromatic hypothesis does generate remarkable errors when determining luminance (of a factor close to 4), and gives rise to a much greater indicated luminance than that actually emitted by a green OLED. Conversely, for an OLED emitting in the blue, the monochromatic assumption leads to a smaller calculated luminance than that found using the more realistic polychromatic configuration. This difference is due to the photoptical eye response.

The importance of this calculation is particularly striking when comparing widely differing color emissions. The general trend based on the monochromatic hypothesis, that green OLEDs luminances are greater than those of blue OLEDs, must be moderated by the fact that a more rigorous calculation using the real polychromatic hypothesis indicates a decrease in the green OLED luminance and an increase in the blue OLED luminance values.

[1] M. Pope, and C. E. Swenberg, *Electronic Processes in Organic Crystals*, (Clarendon, Oxford, (1982).

[2] A. Moliton, *Molecular and Polymer Optoelectronics: From Concepts to Devices*, Springer Series in Optical Sciences (Springer, New York, 2005); and A. Moliton, *Optoélectronique Moléculaire et Polymère: Des Concepts Aux Composants* (Springer, Paris, 2003).

[3] C. W. Tang and S. A. Van Slyke, Appl. Phys. Lett. **61**, 913, (1987).

[4] J. H. Burroughes, D. D. C. Bradley, A. R. Brown, R. N. Marks, K. D. Mackay, R. H. Friend, P. L. Burn, and A. B. Holmes, Nature (London) **347**, 539 (1990).

[5] V. Dentan M. Vergnolle, H. Facoetti, and G. Vériot, C. R. Acad. Sci., Ser IV: Phys., Astrophys. **1**, 425 (2000).

[6] P. E. Burrows, S. R. Forrest, and M. E. Thomson, Curr. Opin. Solid State Mater. Sci. **2**, 236 (1997).

[7] S. Miyata and S. Nalwa, *Organic Electroluminescent Materials and Devices* (Gordon and Breach, New York, 1997).

[8] T. P. Nguyen, P. Molinie, and P. Destruel, in *Organic and Polymer-Based Light-Emitting Diodes*, Vol. 1, Chap. 1, Handbook of Advanced Electronic and Photonic Materials and Devices, edited by H. S. Nalwa (Academic, New York, 2001).

[9] R. Antony, A. Moliton, and B. Ratier, Appl. Phys. B: Lasers Opt. **71**, 33 (2000).

[10] J. Shi and C. W. Tang, Appl. Phys. Lett. **70**(13), 1665 (1997).

[11] F. Desvigne. *Rayonnements Optiques* (Masson, Paris, 1991).

[12] V. Hartel, E. Haseloff, G. Jahn, and G. Suhrke, in *Optoelectronics Theory and Practice*, edited by A. Chappell (McGraw-Hill, New York, 1978).

[13] N. C. Greenham, R. H. Friend, and D. D. C. Bradley, Adv. Mater. (Weinheim, Ger.) **6**, 491 (1994).

[14] D. Troadec. Ph.D. thesis, University of Limoges, 2001.

[15] D. Troadec, G. Vériot, R. Antony, and A. Moliton, Synth. Met. **124**, 49 (2001).